environmental microbiology

Environmental Microbiology (2016) **18**(2), 565–579 doi:10.1111/1462-2920.13130

The complete genome of a viable archaeum isolated from 123-million-year-old rock salt

Salla T. Jaakkola,[1] Friedhelm Pfeiffer,[2] Janne J. Ravantti,[1] Qinggong Guo,[3] Ying Liu,[3] Xiangdong Chen,[3] Hongling Ma,[4] Chunhe Yang,[4] Hanna M. Oksanen[1] and Dennis H. Bamford[1]*

[1]*Department of Biosciences, and Institute of Biotechnology, University of Helsinki, Helsinki, Finland.*
[2]*Department of Membrane Biochemistry, Max Planck Institute of Biochemistry, München, Germany.*
[3]*State Key Laboratory of Virology, College of Life Sciences, Wuhan University, Wuhan, China.*
[4]*State Key Laboratory of Geomechanics and Geotechnical Engineering, Institute of Rock and Soil Mechanics, The Chinese Academy of Science, Wuhan, China.*

Summary

Live microbes have been isolated from rock salt up to Permian age. Only obligatory cellular functions can be performed in halite-buried cells. Consequently, their genomic sequences are likely to remain virtually unchanged. However, the available sequence information from these organisms is scarce and consists of mainly ribosomal 16S sequences. Here, live archaea were isolated from early Cretaceous (~123 million years old) halite from the depth of 2000 m in Qianjiang Depression, Hubei Province, China. The sample was radiologically dated and subjected to rigorous surface sterilization before microbe isolation. The isolates represented a single novel species of *Halobacterium*, for which we suggest the name *Halobacterium hubeiense*, type strain *Hbt. hubeiense* JI20-1. The species was closely related to a Permian (225–280 million years old) isolate, *Halobacterium noricense*, originating from Alpine rock salt. This study is the first one to publish the complete genome of an organism originating from surface-sterilized ancient halite. In the future, genomic data from halite-buried microbes can become a key factor in understanding the mechanisms by which these organisms are able to survive in harsh conditions deep underground or possibly on other celestial bodies.

Received 17 November, 2014; revised 2 March, 2015; accepted 15 March, 2015. *For correspondence. E-mail dennis.bamford@helsinki.fi; Tel. +(358) 2941 59100; Fax +(358) 9386 7170.

Introduction

Microbes inhabit many environments considered extreme. In search of the boundaries of life, researchers have reached even across time-isolating viable microbes from samples of great age, including amber (Cano and Borucki, 1995; Lambert *et al.*, 1998; Greenblatt *et al.*, 1999; 2004), glacial ice (Ma *et al.*, 2000; Christner *et al.*, 2003) and halite (rock salt) (Vreeland *et al.*, 2000; Stan-Lotter *et al.*, 2002; Gruber *et al.*, 2004). Cultivable species of *Bacillus*, *Micrococcus*, *Staphylococcus* and *Streptomyces* have been isolated from 25 to 120 million years of age (MYA) old amber (Cano and Borucki, 1995; Lambert *et al.*, 1998; Greenblatt *et al.*, 1999; 2004). Isolates from ancient ice samples include a wide range of Gram-positive and Gram-negative bacteria (Christner *et al.*, 2003; Sheridan *et al.*, 2003; Miteva *et al.*, 2004), fungi (Ma *et al.*, 2000) and viruses (Castello *et al.*, 1999; Legendre *et al.*, 2014). The oldest ice known to exist on Earth, reaching 8 MYA, can be found from the Antarctic and has been successfully used for microbe isolation (Bidle *et al.*, 2007). Bacteria from amber and ice include both sporulating and non-spore-forming species, but no archaea have been detected. Buried layers of halite, however, harbour both cultivable bacteria and archaea, including members of *Halobacterium*, *Halococcus*, *Halorubrum*, *Haloterrigena*, *Natronobacterium*, *Natronomonas* and *Virgibacillus* (Denner *et al.*, 1994; Vreeland *et al.*, 2000; 2007; Stan-Lotter *et al.*, 2002; Mormile *et al.*, 2003; Gruber *et al.*, 2004; Schubert *et al.*, 2009; 2010a; Gramain *et al.*, 2011). The oldest halite isolation sources are Permian in age (~225–280 MYA): Salado Formation in USA, Bad Ischl in Austria and Boulby potash mine in England (Norton *et al.*, 1993; Vreeland *et al.*, 2000; Stan-Lotter *et al.*, 2002; Gruber *et al.*, 2004).

During prehistoric times, extensive areas on Earth have been covered by salt lakes and seas that now remain as deep salt deposits all over the globe (Zharkov, 1981). Tiny liquid inclusions within the salt carry water offering a habitat for microbes, which have been detected by microscopy from halite crystals of great age (Mormile *et al.*, 2003; Schubert *et al.*, 2009). Even though isolates from ancient halite are numerous, the available sequence data are scarce and consist mainly of 16S rRNA gene sequences. Sequences of some *Virgibacillus* 2-9-3 genes (*gyrB*, *recA*, *splB*, *purL*) and *rpoB´* genes of *Halococcus dombrowskii*

and *Halobacterium noricense* are also available (Maughan *et al*., 2002; Stan-Lotter *et al*., 2002; Gruber *et al*., 2004). Additionally, 16S rRNA gene sequences of uncultured archaea (species of *Halobacterium*) and bacteria (members of β- and γ-*Proteobacteria*) have been amplified from up to 425 MYA-old halite samples (Fish *et al*., 2002; Gramain *et al*., 2011).

A lot of discussion has arisen around the age of these isolates. The halite age can be estimated by radiological methods and geological analyses of the sampling sites (Vreeland *et al*., 2000). The age of the brine inside the liquid inclusions can be determined by measuring ion ratios by laser ablation inductively coupled plasma mass spectrometry (LA-ICP-MS) or environmental scanning electron microscope X-ray energy dispersive analysis techniques (Fish *et al*., 2002; Satterfield *et al*., 2005). To eliminate the possibility of microbial contamination during sample handling, stringent sterilization procedures have been developed and applied (Rosenzweig *et al*., 2000; Gramain *et al*., 2011; Sankaranarayanan *et al*., 2011).

Somehow these cells remain viable despite being in a nutrient- and oxygen-depleted environment for millions of years. In studies on bacterial spores, the estimated time for their survival inside halite ranged from 109 to over 250 million years (Kminek *et al*., 2003; Nicholson, 2003). Archaea are not known to sporulate, but possibly form resting cells with minimal metabolism (Grant *et al*., 1998). Rod-shaped or polymorphic cells of *Halobacterium salinarum*, *Hbt. noricense* and *Haloferax mediterranei* divide into small spherical cells when introduced to very low water activity (Fendrihan *et al*., 2004; 2012). These spherical cells, which regain their original morphology in rich medium, have a reduced ATP content and a long lag-phase, thus resembling bacterial spores (Fendrihan *et al*., 2012). Round, miniaturized cells have also been detected inside ancient salt crystals, and they predominate among cells in ancient ice samples (Sheridan *et al*., 2003; Miteva *et al*., 2004; Schubert *et al*., 2009). These small coccoid cells might be archaeal resting cells. In addition, *Halobacterium* cells isolated from middle to late Eocene halite grew as tiny, clustered cocci instead of rods typical of *Halobacterium* species (Jaakkola *et al*., 2014). It seems that archaea in general deploy a range of survival methods despite not being able to sporulate: desiccated cells of *Methanosarcina barkeri* have an enhanced tolerance towards high temperatures, radiation and oxygen (Anderson *et al*., 2012), and *Methanosarcina soligelidi*, an isolate from Siberian permafrost, has remarkable resistance towards desiccation, freezing and thawing (Wagner *et al*., 2013).

To survive over extended periods of time, cells need to maintain their DNA intact. Although thick layers of halite and other minerals provide efficient protection from radiation (Fendrihan *et al*., 2009), and high intracellular salt concentration inhibits depurination of DNA (Marguet and Forterre, 1998; Shahmohammadi *et al*., 1998), active DNA repair mechanisms are needed. Indeed, metabolical activity and DNA repair have been detected in bacteria inside permafrost (Johnson *et al*., 2007), implying those processes may be ongoing in halite-buried microbes as well. All haloarchaea tested to date are polyploid, with chromosome copy numbers ranging from 6 to 25, including freshly isolated species from middle to late Eocene halite (Soppa, 2011; Jaakkola *et al*., 2014). Polyploidy has been suggested to aid in DNA maintenance of buried cells (Soppa, 2013; Jaakkola *et al*., 2014), as it facilitates DNA repair and mutation control (Zerulla *et al*., 2014). The extra chromosomes also serve as storage molecules, which may help in recovering from nutrient depletion (Zerulla *et al*., 2014). The energy and nutrients needed for DNA repair and other metabolic activities are most likely derived from organic matter inside the liquid inclusions in halite. Especially, glycerol, produced by the halophilic algae *Dunaliella salina*, is an important nutrient in hypersaline environments, and *Dunaliella* cells have been shown to co-occur with viable archaea and bacteria inside halite sediments (Schubert *et al*., 2010b). The levels of intracellular glutamate are also high in haloarchaea, providing a carbon source for the cells (Kokoeva *et al*., 2002).

In this study, we isolated microbes representing a novel species of *Halobacterium* from a surface-sterilized 123 MYA bore core halite sample obtained from the depth of 2000 m from a salt mine in Qianjiang, Hubei Province, China. The isolated species is closely related to *Hbt. noricense* isolated from Permian halite (Gruber *et al*., 2004). The complete genome of the type strain, JI20-1, was sequenced to gain a deeper understanding of the relatedness of deeply buried microbes to modern ones.

Results

The halite sample was 123 MYA and originated from early Cretaceous era

Jianghan Basin is a large, saline lacustrine inland basin in Hubei Province, China (Fig. 1A), with an area of 27 920 km^2. It was formed during the early Cretaceous (100–145 MYA) and has evolved from a downfaulted basin to a regionally subsiding one during the Quaternary Period (0–2.6 MYA) (Philp and Zhaoan, 1987; Xiang *et al*., 2007). The basin consists of four saliferous depressions: Jiangling, Qianjiang, Xiaoban and Yunying. The Qianjiang Depression (Fig. 1B) is the largest lacustrine salt deposit in China with an area of 2610 km^2 (Philp and Zhaoan, 1987; Matzko, 1995), and the salt caverns in the area are an abundant source of oil and gas (Philp and Zhaoan, 1987; Philp *et al*., 1991; Du *et al*., 2012; Ma *et al*., 2012). The southern part of Qianjiang Depression, called Diaotikou syncline, has been forming from Cretaceous

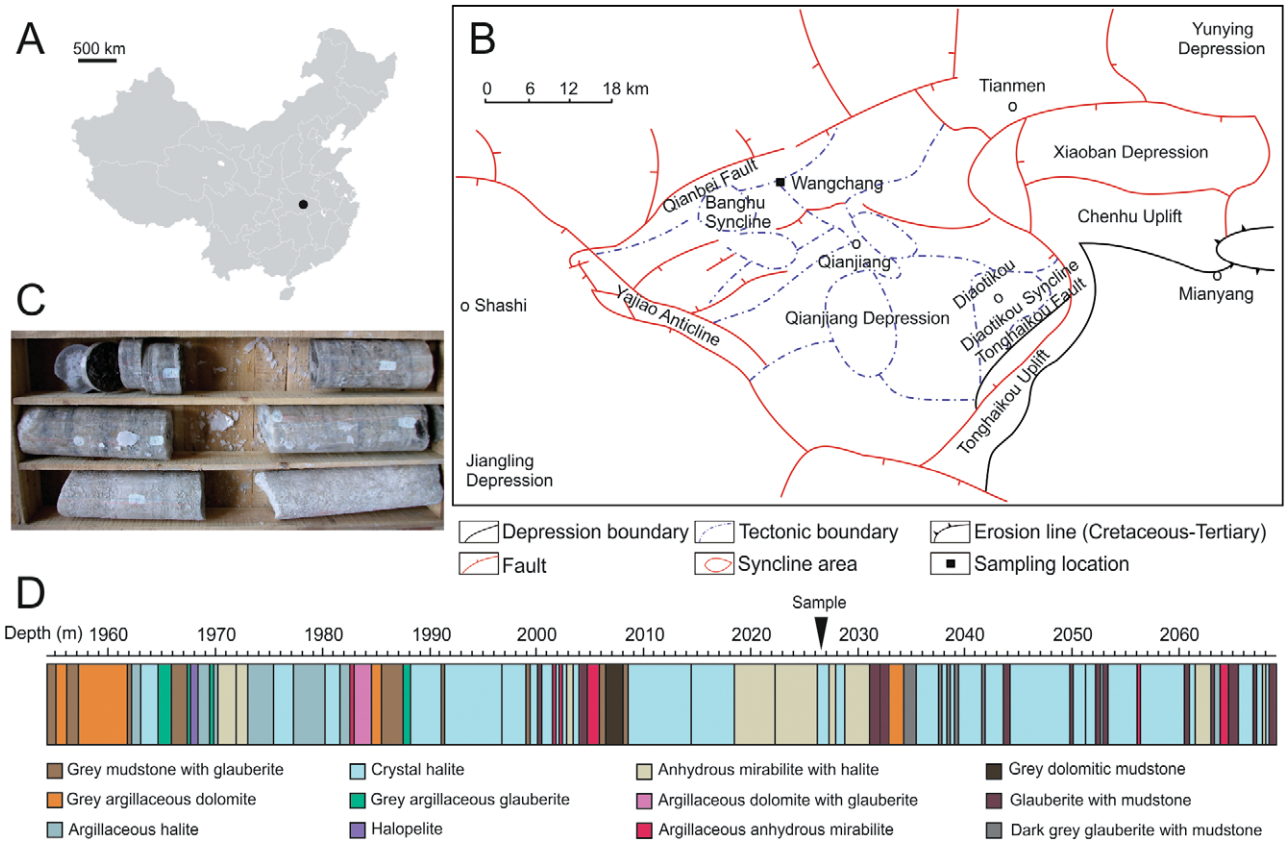

Fig. 1. The sampling site, Wangchang (30°29′N, 112°58′E, black circle), Hubei Province, is shown on the maps of (A) China and (B) Qianjiang Depression. (C) Drill core subsections and (D) the stratigraphic profile of the sampling site are shown. The depth of the sample used in this study is marked with a black arrowhead in (D). Map of China is from Wikimedia Commons. Data in (B) and (D) was obtained from Research Institute of Exploration and Development, Jianghan Oilfield Company, SINOPEC.

(66–145 MYA) to middle Eocene (38–48 MYA). Its paleotopography is shallow in the north and deep in the south, with a subsidence centre in front of Tonghaikou fault. The depression in the northern part, Banghu syncline, has formed during middle and late Eocene (34–41 MYA). Its paleotopography is deep in the north and shallow in the south, with a subsidence centre in the front of Qianbei fault. The Qianjiang Formation consists of 193 distinct layers of salt and other materials. The burial depths of the salt layers are generally between 870 and 3600 m, and the area of solid halite is 1800 km^2. The thickness of most monolayers varies between 4 and 35 m, and the thickest one is 84.5 m. A drill core (Fig. 1C) was taken from Wangchang in Qianjiang Depression (Fig. 1B), and a subsection from 2026.51 to 2026.80 m consisting of crystal halite was used for this investigation (Fig. 1D). The age of the drill core sample was estimated using U-Pb isotope dating of detrital zircons. The radiological dating identified different populations of zircons from the crystal (Table S1). The youngest zircons were 123 ± 2.3 MYA, and the oldest ones were 2268 ± 36.1 MYA, placing the age of the crystal around 123 MYA (Fig. S1).

A 53 g piece of the drill core sample was selected for microbe isolation. The crystal consisted of grainy halite with small mudstone particles, and had a thin rock layer at one side (Fig. S2A). Fractions cut from the crystal were studied under light microscopy. Liquid inclusions were detected that had an irregular or cubic form, and a diameter ranging from ~3 to 30 μm (Fig. S2B–D).

Eight cultivable microbes were isolated from the surface-sterilized samples

Before microbe isolation, the halite crystal surface was sterilized. Samples of solutions (excluding HCl and NaOH) used in the process were plated, resulting in no growth. Several subsections were cut from the inside of the surface-sterilized crystal, avoiding any material that had been in contact with the surroundings. Two individual crystal aliquots were handled separately and used for microbe isolation. After 21 days of incubation, a total of eight isolates of red, phenotypically similar colonies were obtained, which were named from JI20-1 to JI20-8 in numerical order. JI20-1 was the only isolate from the other

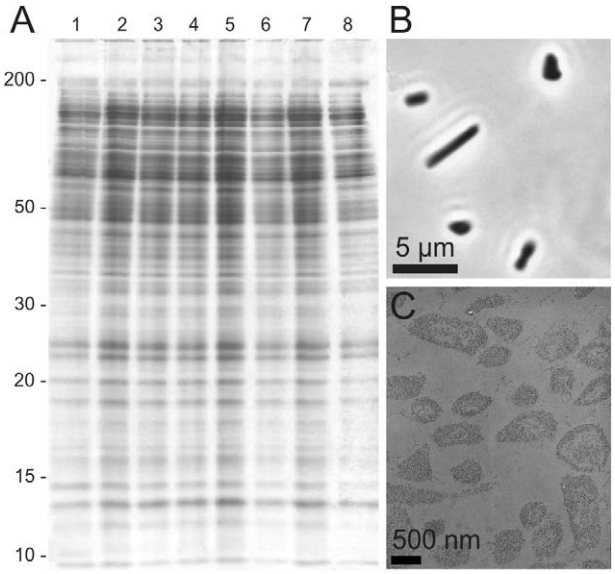

Fig. 2. (A) Whole cell protein patterns of isolated strains JI20-1 to JI20-8 analysed by SDS-PAGE and Coomassie staining (lanes 1–8). Molecular mass standards for (A) are shown on left. (B) Light microscopy and (C) thin section transmission electron microscopy of isolate JI20-1.

crystal aliquot. The whole cell protein patterns of the pure cultures of the isolates were similar, suggesting they belong to a single species (Fig. 2A). The cells appeared as rod shaped (2–5 μm long and 1 μm thick) and motile (Fig. 2B and C). Occasional coccoid and irregularly shaped cells were also seen. No viruses could be isolated from the halite sample.

Isolate JI20-1 needed NaCl for growth, and grew optimally in the presence of 2.5 M NaCl (Fig. S3A). Magnesium, however, was not necessary for growth, and the optimum was at 0–0.1 M $MgCl_2$ (Fig. S3B). On plate, JI20-1 could grow at temperatures from 22 to 50°C. In liquid, the fastest growth was detected at 45°C, but none at 50°C (Fig. S3C). All eight isolates grew similarly under optimized conditions (Fig. S3D).

The isolates represent a novel species of the genus Halobacterium

The complete genome sequence of JI20-1 was determined, and draft genomes for the other seven isolates (JI20-2- JI20-8) were prepared (Table S2). Predicted open reading frames (ORFs) in the draft genomes were also present in JI20-1, and no significant genomic differences were found between these isolates. The 16S rRNA and *rpoB′* gene sequences of all eight isolates were identical (data not shown). JI20-1 was used as a representative of the JI20-isolates in phylogenetic analyses based on the 16S rRNA and *rpoB′* gene sequences (Fig. 3). It grouped with known species of *Halobacterium*, and the closest match to a known species was to *Halobacterium noricense*, an isolate from Permian Alpine rock salt from the depth of 470 m (Gruber *et al*., 2004), with 99% and 96% identities of 16S rRNA and *rpoB′* genes respectively. The JI20-1 16S rRNA gene was 99.9% identical to the partial 16S rRNA genes of *Halobacterium* sp. YI80-1 and YI80-2, which originate from surface-sterilized middle to late Eocene halite (38–41 MYA) near the Qianjiang Depression (Jaakkola *et al*., 2014). The JI20-1 16S rRNA gene identity to the other members of *Halobacterium* (*Halobacterium* sp. DL1, *Hbt. jilantaiense*, *Hbt. salinarum* and *Hbt. piscisalsi*) was 97%.

Whole-cell protein patterns of *Hbt. noricense* and JI20-1 differed significantly from each other (Fig. S4). Furthermore, DNA–DNA hybridization re-association value between *Hbt. noricense* and JI20-1 was 43.0%. As the cut-off value of 70% is commonly used for distinguishing different species (Stackebrandt and Goebel, 1994), we conclude that our isolate is a novel species, for which we propose the name *Halobacterium hubeiense*, type strain being *Hbt. hubeiense* JI20-1.

Genome of Halobacterium hubeiense

Halobacterium hubeiense has a genome organization typical of halophilic archaea. The 3 130 345 bp genome (Fig. 4A) consists of one high guanine-cytosine (GC) chromosome (Fig. 4B) and three smaller replicons, pSTJ001, pSTJ002 and pSTJ003 (Fig. 4C–E), with a lower GC content. The three smaller replicons were considered to be megaplasmids instead of minichromosomes because no genes that were indispensable for the microbe viability were identified.

The *Hbt. hubeiense* genome had 3437 putative protein-coding genes (Hhub_1001-3766 in the chromosome, Hhub_4001-4354 in pSTJ001, Hhub_5001-5181 in pSTJ002 and Hhub_6001-6133 in pSTJ003), with an average coding density of 90% (~91% in the chromosome and 82–83% in the plasmids) (Fig. 4A). The starting codon was ATG in 84.4% of the genes, GTG in 15.4%, and TTG in 0.2%. A total of 57 genes coding for stable RNAs were identified. A single rRNA operon resided in the chromosome, and a complete set of tRNAs (47 genes) was present. There were three copies of tRNA-Glu, and one of them resided in pSTJ003 (Fig. 4B and E). The origin of replication in the chromosome (Fig. 4B) was preceded by a set of three genes (*oapABC*), which are conserved in all haloarchaea, but have unknown functions. These genes point away from the origin, a configuration that is found in all haloarchaea. The chromosome ring was opened C-terminal to *oapC* (Hhub_1001), as in the *Natronomonas moolapensis* genome (Dyall-Smith *et al*., 2013), to highlight the close association of the *oapABC* genes with the replication origin. Gene for an Orc1/Cdc6-type DNA

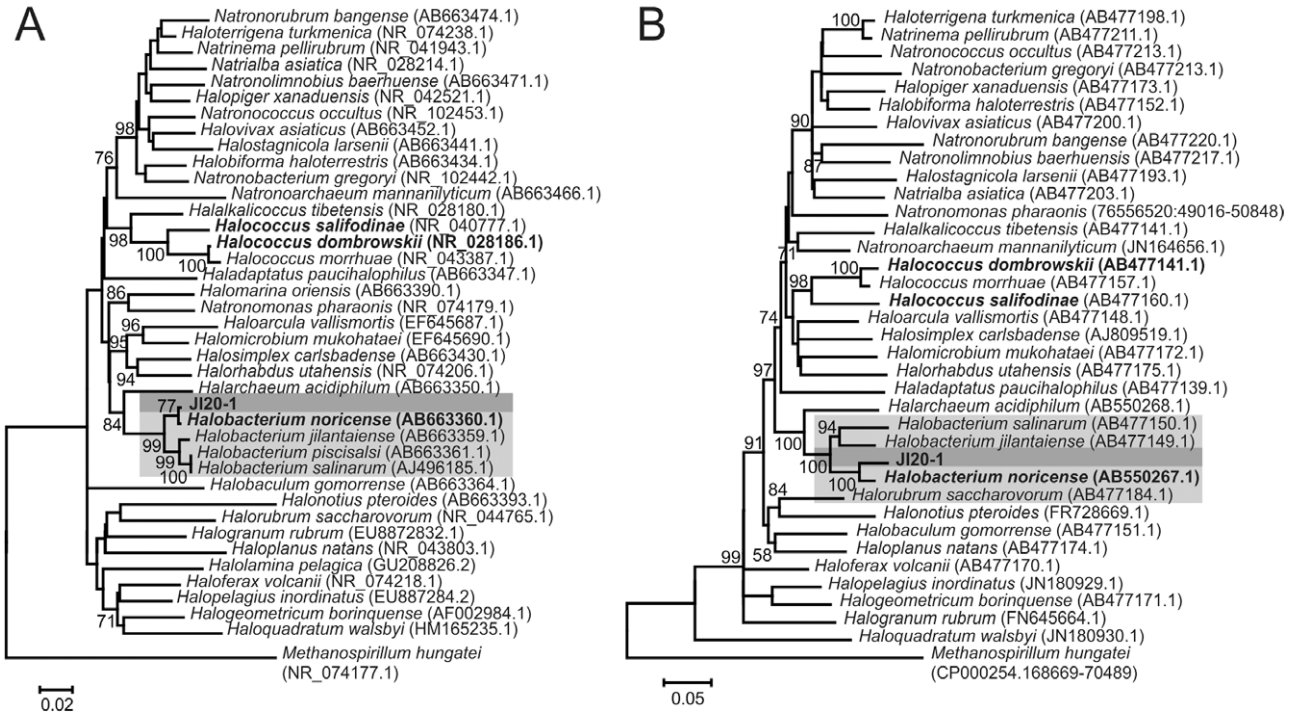

Fig. 3. The maximum likelihood phylogenetic trees based on (A) 16S rRNA and (B) *rpoB′* gene sequences. Members of *Halobacterium* are in light grey and isolate JI20-1 in dark grey. The names of the isolates from surface-sterilized ancient rock salt are bolded. The bars represent inferred substitutions per nucleotide position.

replication protein resided on the other side of the origin, pointing away from it. Orc1/Cdc6 proteins were coded from each replicon (four in the chromosome, two in pSTJ001 and pSTJ002, and one in pSTJ003). Genes coding for basal transcription factors TBP and TFB, and cell division related Orc1/Cdc6 and FtsZ, are typically found in multiple copies in haloarchaeal genomes (Berquist and DasSarma, 2003; Soppa, 2006). In *Hbt. hubeiense*, each replicon had one TBP coding gene. There were seven TFB-coding genes in the chromosome, and one in each plasmid, and seven copies of the *ftsZ* gene resided in the chromosome.

The proteome isoelectric point (pI) was low (5.0), which is typical of halophiles (Paul *et al.*, 2008). Haloarchaea generally use intracellular potassium as an osmoprotectant (da Costa *et al.*, 1998). This is believed to be connected to proteome acidity, but *Hbt. hubeiense* also had a gene for a glycine betaine transporter (Hhub_2282), suggesting a possible use of compatible solutes in addition to the salt-in strategy. The cells were motile, as observed by microscopy (Fig. 2B), and genes for flagellin were found accordingly. Transducer genes for chemotactic, aerotactic and phototactic movement were also present. Genes for utilizing glycerol, an important carbon source for halite-buried microbes, were identified.

A total of 2295 (66.8%) of the putative gene products were assigned a function based on homology (Fig. 4F). The largest group with a specific function (7.7%) was small molecule transport (Fig. 4F). No clear functional segregation between the replicons was detected, but some trends could be seen (Fig. 4B–E). The plasmids contributed little to metabolical activity. They also had a higher percentage of genes with unknown functions (46.4–50.6%) than the chromosome (29.4%). The plasmids pSTJ001 and pSTJ003 carried a high amount of transporter genes (10.7 and 8.1% respectively). All protein secretion genes resided in the chromosome. Genes for a complete Sec-system were identified, and three genes (*tatA*, *tatC1* and *tatC2*) for the twin arginine export pathway. A tat-export signal was predicted in 119 genes. A signal-recognition particle pathway was also present.

Comparison of Hbt. hubeiense *to modern haloarchaea*

Dot-plot analyses comparing *Hbt. hubeiense* JI20-1 genomic sequence to those of *Hbt. salinarum* R1 or *Halobacterium* sp. DL1 revealed a high amount of synteny between the chromosomes of these species, although some inversions were present (Fig. 5). The *Hbt. hubeiense* plasmids instead were not related to the plasmids of these species.

Most of the *Hbt. hubeiense* genes had homologues in known haloarchaeal genomes (3001, 87.3%, requesting a BLASTp e-value better than e-20). Among 102 complete proteomes from the taxonomic group Halobacteriaceae,

A

Replicon	Length (bp)	GC%	Coding DNA	CDSs[a]	RNAs[b]	ORFans
Chromosome	2,510,607	68.4	91.1%	2765	52	95
pSTJ001	349,522	56.0	82.7%	356	4	34
pSTJ002	157,757	59.3	82.7%	181	0	3
pSTJ003	112,459	56.5	82.2%	135	1	8
Total	3,130,345	61.0	89.6%	3437	57	138

[a]protein coding genes, [b]stable RNA coding genes

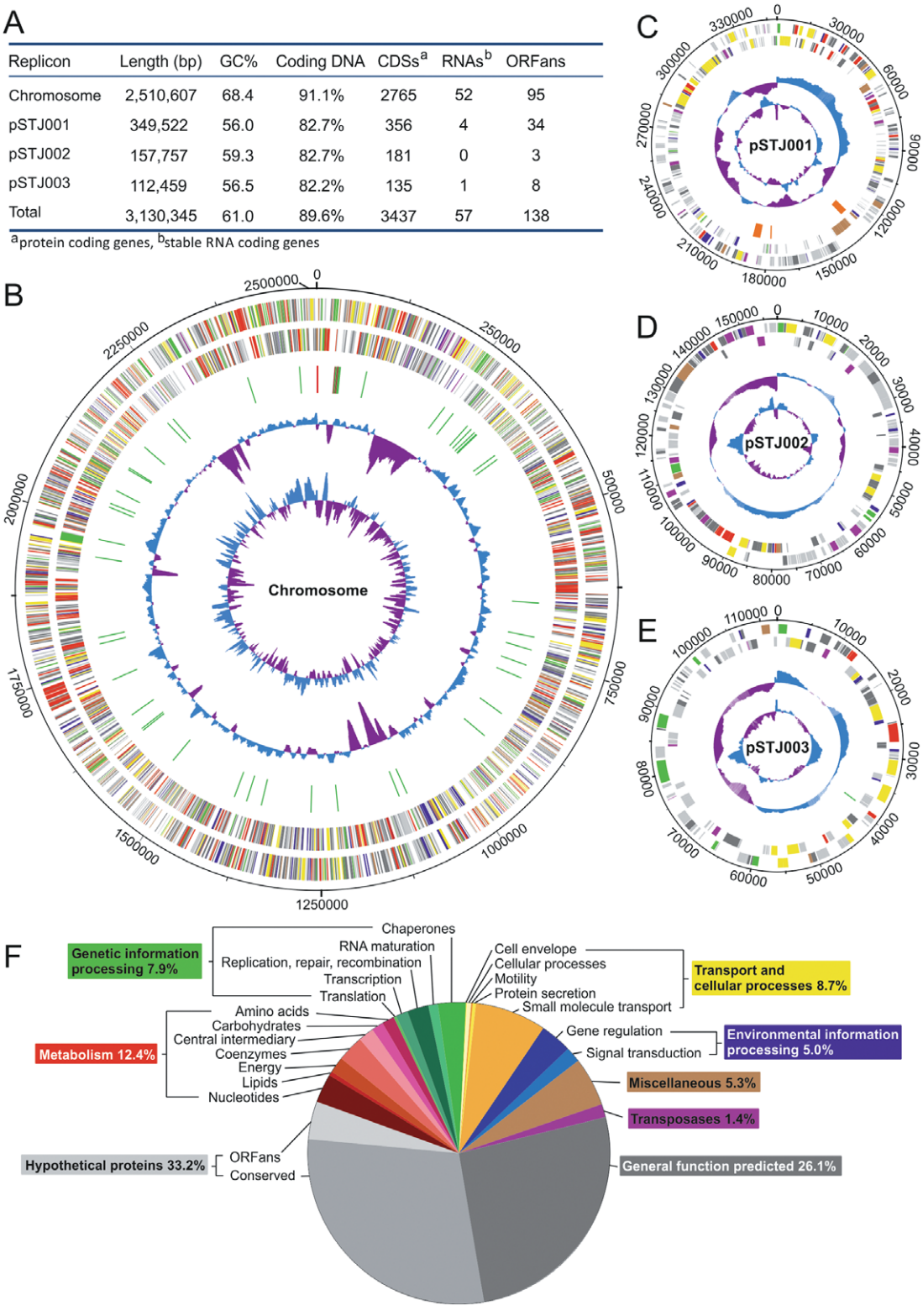

Fig. 4. The *Halobacterium hubeiense* genome.
A. Chromosome and plasmid properties.
B–E. Graphical maps of the replicons, where the graphs from outside towards inside represent: (i) sequence coordinates (bp); (ii) protein-coding genes on the forward strand; (iii) protein-coding genes on the reverse strand; (iv) origin of replication (red), tRNA (green), rRNA genes (brown) and CRISPR arrays (orange); (v) GC content; (vi) GC skew.
F. Gene products divided in functional classes. The ORFs in (B–E) are coloured according to the colours of functional category labels in (F).

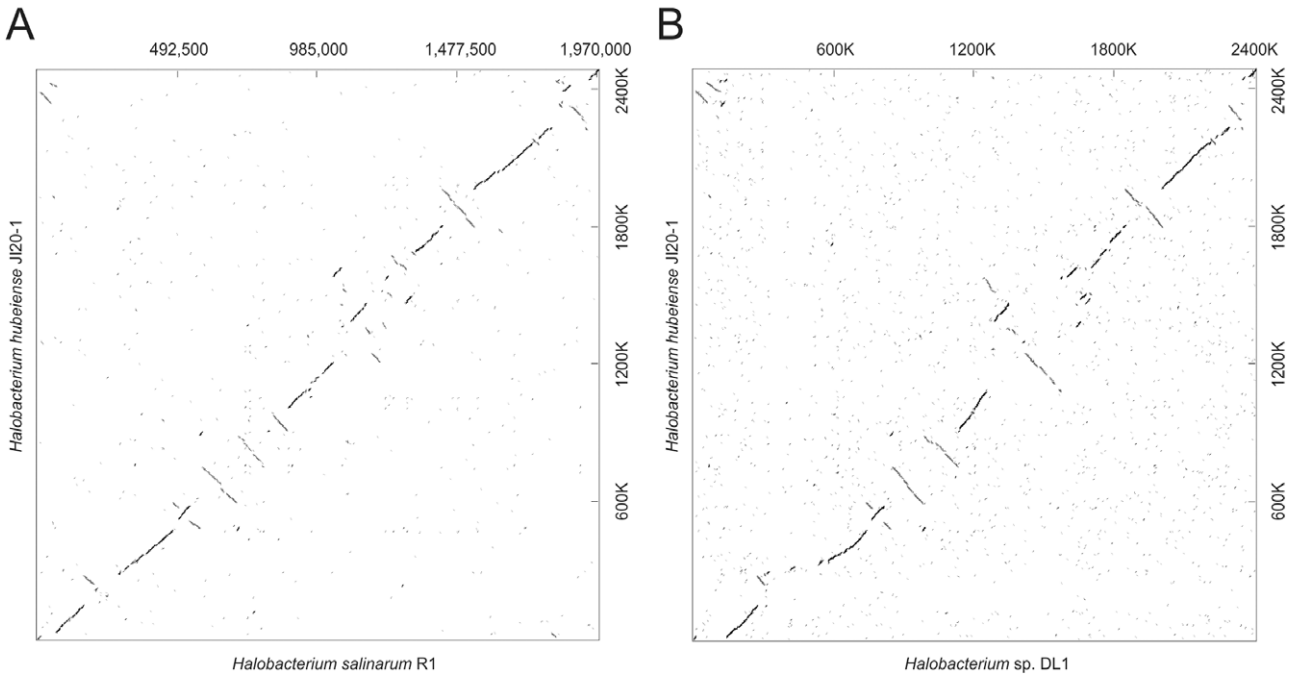

Fig. 5. Dot-plots comparing the *Hbt. hubeiense* JI20-1 chromosome to (A) *Hbt. salinarum* R1 and (B) *Halobacterium* sp. DL1 chromosomes. The sequence positions (bp) are shown on top and right. The origin associated gene *oapC* or its homologue was used as a starting point for all genomes (16 bp in JI20-1, 1 792 952 bp in R1 and 2 845 106 bp in DL1).

the three species of *Halobacterium* (*Hbt. salinarum* R1 and NRC-1, and *Halobacterium* sp. DL1) have an especially high number of homologues in *Hbt. hubeiense* (60.6–65.3%) compared with those in species from other genera (*Halarchaeum* up to 36.9% and *Halorubrum* up to 29.1%) (Table 1). The chromosome had three distinct low GC% islands (Fig. 4B), which all had an increased amount of genes related to other haloarchaea than species of *Halobacterium*. On genus level, 2170 *Hbt. hubeiense* ORFs (63%) were homologous to genes in species of *Halobacterium*, 1336 (39%) to *Halorubrum* genes, 1297 (38%) to *Haloferax* genes, 1246 (36%) to *Natrinema* genes and 1242 (36%) to *Haloarcula* genes. These five were the most closely related genera.

The ORFs in the *Hbt. hubeiense* chromosome were preferentially related to *Halobacterium* ones, covering 57–60% of the reference organism proteomes (1391–1870 homologues) (Table 1). There was a high number (1022) of homologues to *Natrinema pellirubrum* proteins, but because this organism has a very large proteome, the *Hbt. hubeiense* homologues covered only 20% of its proteome (Table 1). The ORFs in the *Hbt. hubeiense* plasmids were more closely related to other species than those belonging to *Halobacterium* (Table 1). Of the pSTJ001 ORFs, only 11–13% had homologues in *Halobacterium* proteomes, but 25% had homologues in *Haloarcula japonica* or *N. pellirubrum*. Of pSTJ002 ORFs, 27–39% had homologues in *Halobacterium* proteomes, but 80% were homologous to *N. pellirubrum*, and 10–23% of the pSTJ003 ORFs had homologues in *Halobacterium* proteomes, but 56% were homologous to *Haloarcula marismortui* and 55% to *Har. japonica* (Table 1). Interestingly, pSTJ003 carried a continuous 45 366 bp sequence (~40% of pSTJ003) with 88.6% identity to *Har. marismortui* plasmid pNG600. This part of the plasmid also carries the tRNA gene.

There were some notable differences in the genes of *Hbt. salinarum* and *Hbt. hubeiense*. *Halobacterium hubeiense* did not possess a gene for halorhodopsin or bacteriorhodopsin, present in *Hbt. salinarum*, but genes for the phototactic response regulating sensory rhodopsin II and its adjacent transducer were present. Genes for gas vesicles, found in *Hbt. salinarum*, were not identified. Unlike *Hbt. salinarum*, *Hbt. hubeiense* did carry genes for reducing nitrate to nitrite and further to ammonia (Hhub_2082, Hhub_2083) and is probably capable of nitrate assimilation. *Halobacterium hubeiense* had a larger potential for small molecule transport: 263 genes coded for transport system proteins, whereas the corresponding number in *Hbt. salinarum* R1 is only 181 (Pfeiffer *et al*., 2008b).

Halobacterium hubeiense coded for five DNA polymerases: PolB, PolB2, PolD, PolX and PolY, but in *Hbt. salinarum* PolX is not present. *Halobacterium hubeiense* had also genes for multiple DNA repair systems, including a deoxyribodipyrimidine photolyase,

Table 1. Relatedness of the *Hbt. hubeiense* JI20-1 proteome to other haloarchaeal proteomes.

Reference organism			Number of homologues in *Hbt. hubeiense*[a]				Relatedness to *Hbt. hubeiense*	
Species and strain	Organism tag	Total ORFs	Total	Chromosome	pSTJ001	pSTJ002	pSTJ003	Serial no.[b]	Homologues in reference (%)
Halobacterium salinarum (ATCC 29341/DSM 671/R1)	HALS3	2577	**1682**	**1534**	46	71	31	1	65.3
Halobacterium salinarum (ATCC 700922/JCM 11081/NRC-1)	HALSA	2426	**1505**	**1391**	39	49	26	2	62.0
Halobacterium sp. DL1	9EURY_#1	3265	**1977**	**1870**	38	55	14	3	60.6
Halarchaeum acidiphilum (MH1-52-1)	9EURY_#2	2706	999	933	38	23	5	4	36.9
Halorubrum hochstenium (ATCC 700873)	9EURY_#3	2931	853	748	36	57	12	5	29.1
Halorubrum litoreum (JCM 13561)	9EURY_#4	3014	870	739	32	**77**	22	6	28.9
Halorubrum saccharovorum (DSM 1137)	9EURY_#5	3231	904	771	44	59	30	7	28.0
Haloferax denitrificans (ATCC 35960)	9EURY_#6	3774	1036	934	66	22	14	8	27.5
Haloarcula japonica (DSM 6131)	HALJP	4255	1133	894	**88**	76	**75**	11	26.6
Natrinema pellirubrum (DSM 15624/JCM 10476/NCIMB 786)	NATP1	5026	1301	1022	**87**	**145**	**47**	18	25.9
Natrinema giari (JCM 14663)	9EURY_#7	4056	1016	825	54	**121**	16	26	25.0
Haloarcula marismortui (ATCC 43049/DSM 3752)	HALMA	4237	1023	845	50	52	**76**	41	24.1
Haloferax volcanii (ATCC 29605/DSM 3757/DS2)	HALVD	4811	1129	999	**75**	40	15	46	23.5

a. Three highest homologue counts for the complete *Hbt. hubeiense* JI20-1 genome (total) and each replicon are bolded.
b. Based on the percentage of *Halobacterium hubeiense* homologues in the reference organis.

uvrABC nucleotide excision repair system, mutS/L system for mismatch repair and a rad50/mre11 system for repairing double-strand breakages. There were no significant differences to DNA repair systems in *Hbt. salinarum*, which, however, is known to be highly resistant to DNA damage (Kottemann *et al*., 2005). The set of genes involved in nucleotide metabolism and translation were also very similar in these two species.

Clustered regularly interspaced short palindromic repeats - CRISPR associated protein (CRISPR-Cas) system

A CRISPR-Cas system of type I-B (also called Tneap–Hmari or CASS7) typical of halophilic archaea was identified in pSTJ001. Four CRISPR arrays (Fig. 4C) carried 113 spacers (33–47 bases long). Some of the spacers had matches to known viral sequences in the NCBI nucleotide database (Table S3). No integrated viruses could be found in the genome. There is no CRISPR-Cas system in the genome of *Hbt. salinarum*, but homologous Cas-proteins and one CRISPR array resembling *Hbt. hubeiense* CRISPR array 1 were identified in the genome of *Halobacterium* sp. DL1. The *Hbt. hubeiense* CRISPR array 1 direct repeat (DR), which is 30 bases long, is nearly identical to the DR of *Halobacterium* sp. DL1, with only two single base mutations. *Halobacterium* sp. DL1 CRISPR array contained 54 spacers, which is four more than in the *Hbt. hubeiense* CRISPR array 1. There was no significant identity between the spacers. BLAST analysis of the *Hbt. hubeiense* DRs against CRISPRdb database (Grissa *et al*., 2007a) revealed the array 1 DR being homologous to haloarchaeal DRs, but the DRs of the three other arrays had no matches. Some of the *Hbt. hubeiense* spacers matched the CRISPRdb sequences: the spacer 46 of array 1 and spacer 47 of array 4 had hits to *Hfx. mediterranei*, which were the only haloarchaeal ones.

Transposable elements

There were 48 transposase genes in the *Hbt. hubeiense* genome, of which 18 were predicted to be non-functional. Majority of the transposon genes (33) resided in the plasmids, possibly contributing to plasmid plasticity. Most transposases (28) were of the IS1341 type, including short remnants (Dyall-Smith *et al*., 2011). The transposons were highly diverse, occurred in very low copy numbers, lacked inverted terminal repeats and did not cause target duplications. Four transposons carried one IS200-type transposase and an adjacent IS1341-type transposase. In addition, *Hbt. hubeiense* contained a number of palindrome-associated transposable elements, which have termini reminiscent of IS1341-type transposons, but do not carry a transposase gene (Dyall-Smith *et al*., 2011).

A large number of transposable elements is found in the genome of *Hbt. salinarum*, leading to high genome plasticity (DasSarma *et al*., 1988; Pfeifer and Blaseio, 1990), which is exemplified by differences occurring between *Hbt. salinarum* NRC-1 and R1 genomes. However, most of the canonical transposons showing signs of mobility in *Hbt. salinarum* were either absent or present as single copies in *Hbt. hubeiense*. Based on this observation, the *Hbt. hubeiense* genome does not seem to be prone to change.

Discussion

Bacteria and archaea from rock salt sediments up to the Permian age (225–280 MYA) have been isolated from several locations globally, but no studies so far have provided sequence information beyond few individual genes. Unassembled genome data for *Halosimplex carlsbadense* is available, but despite this organism originating from a Permian halite formation, it has been isolated from an unsterilized sample, and thus cannot be considered ancient (Vreeland *et al*., 2002). In this study, we isolated cultivable halophilic archaea, which all represented a single species of genus *Halobacterium*, from surface-sterilized rock salt deposited during the early Cretaceous (~123 MYA). Based on genome sequence comparison and DNA–DNA hybridization, the isolated species did not belong to any of the known species of *Halobacterium*, and the name *Hbt. hubeiense* is suggested, referring to the site of sampling in Hubei province, China. *Halobacterium hubeinese* is now the first microbial species isolated from an ancient source, for which a complete genome sequence is available, providing valuable data into studying halite-buried archaea. The genome is unexpectedly similar to modern haloarchaeal genomes, changing the view we have of halite-buried microbes.

The radiologically estimated age of our sample (~123 MYA, Fig. S1) was in accordance with the age of the Jianghan Basin (~100–145 MYA), and the sampling site was undisturbed and covered by intact sediment layers. The sample contained liquid inclusions (Fig. S2), enabling the presence of viable microbes. The concentration of cultivable microbes was very low (1–8 cfu g^{-1}), although some viable cells could have still resided in the sample but were not cultivable by our methods and/or in aerobic conditions. Contaminations during sample handling were excluded by rigorous surface sterilization in a sterile environment. In addition, our isolation process and results could be repeated. The slow growth of the cells (visible colonies only after 21 days) also points to dormancy of the cells, indicative of entombment. Thus we conclude that the isolates did originate from the early Cretaceous halite. This is further supported by the relatedness of *Hbt. hubeiense* to Permian (225–280 MYA) *Hbt. noricense* and middle to late Eocene (38–41 MYA) *Halobacterium* sp. YI80-1 and YI80-2 from Yunying Depression in China, located close to the Qianjiang Depression (Gruber *et al*., 2004; Jaakkola *et al*., 2014). *Halobacterium* sp. YI80-1, as well as two *Halolamina* isolates from the same site, are shown to be polyploid, which might contribute to the longevity of halite-buried microbes by enhancing mutation control and DNA repair (Jaakkola *et al*., 2014). Polyploidy is also common in surface haloarchaea (Breuert *et al*., 2006). Therefore it is likely that *Hbt. hubeiense* also has multiple copies of its genome.

Species of *Halobacterium* and their 16S rRNA genes are common in rock salt of great age (Norton *et al*., 1993; Fish *et al*., 2002; Mormile *et al*., 2003; Gruber *et al*., 2004; Vreeland *et al*., 2007; Gramain *et al*., 2011), and the cells are well adapted for survival during prolonged entombment (Gramain *et al*., 2011). *Halobacterium salinarum* has effective DNA repair mechanisms (McCready, 1996; Baliga *et al*., 2004). *Halobacterium* sp. NRC-1 is highly resistant towards damage caused by desiccation and radiation (Kottemann *et al*., 2005; DeVeaux *et al*., 2007). The DNA is protected by bacterioruberin and high intracellular KCl, which reduce oxidative damage (Shahmohammadi *et al*., 1998; Asgarani *et al*., 1999). High expression level of single-stranded DNA-binding protein has also been detected in radiation-resistant mutants of *Halobacterium* sp. NRC-1 (DeVeaux *et al*., 2007). The *Hbt. hubeiense* genes related to DNA repair were the same as in *Hbt. salinarum*, although it is possible that there are DNA repair system proteins that are yet unknown. However, it is plausible that the detected DNA repair mechanisms coupled to polyploidy are enough to enable prolonged survival inside halite. The conservation of the DNA repairing genes underlines the importance of their function. Periodical dry seasons, and even complete desiccation affect many hypersaline lakes. Becoming encased in halite is common, and it protects haloarchaeal cells from environmental stress during the dry season. Hypersaline environments are also exposed to high levels of UV radiation, requiring efficient DNA maintenance in halophiles.

Interestingly, albeit isolated from an ancient source, *Hbt. hubeiense* does not display significant genomic differences to surface haloarchaea. Most (~63%) genes of *Hbt. hubeiense* are highly homologous to known *Halobacterium* genes, as well as to genes of other halophilic archaea (Table 1). Especially the plasmid pSTJ003 is very closely related to *Har. marismortui* plasmid pNG600. These results do not support the idea of the ancient rock salt isolates being notably different from modern halophiles (Grant *et al*., 1998). Hypersaline habitats are characterized by high concentration of nutrients and a low diversity of species, leading to decrease in competition. Both growth rates and predation are low. Adding the effect of polyploidy-related mutation control,

evolution of halophiles is slow. The buried cells should not evolve, as they are not likely to exhibit growth or cell division. We believe that this alone does not explain the similarity of subsurface sediment and free-living microbes, and the observed sequence similarity between surface and subsurface microbes infers some type of species exchange between these two habitats.

The possibility of buried halite becoming contaminated by outside microbes has been presented (McGenity *et al*., 2000). The topmost mineral layers dissolve by surface waters and become inhabited by new microbes (Gramain *et al*., 2011). However, the permeability of intact halite is very low (Beauheim and Roberts, 2002). At Permian Salado formation in New Mexico and Texas, USA, it has been calculated that it would take water more than 30 million years to flow 1 m through halite (Powers *et al*., 2001). It does not seem plausible that salt accumulations all around the globe would have been externally contaminated at the depths of hundreds of meters by related species. Whereas the halite layers are difficult to enter, they are easy to exit. Deposited salt is exposed and dissolved due to natural geological processes and human action, such as mining, releasing buried microbes in the process. In practice, the surface populations contain microbes released from halite of different ages, including both bedded salt and modern halite crystals. This continuous mixing of halite-encased microbes to contemporary populations could explain the marginal differences observed between ancient rock salt isolates and the so-called modern ones. Lateral gene transfer between species and genera, where large amounts of genomic material is exchanged, is common among halophiles (Grant *et al*., 1998; Naor *et al*., 2012; DeMaere *et al*., 2013). Genes of the microbes released from underground could easily spread in the haloarchaeal population. It has been suggested that hypersaline waters can be viewed as a network of 'islands' loosely connected to each other (Atanasova *et al*., 2012). We should begin to view rock salt deposits as one part of this network, contributing to the microbial flora of hypersaline environments.

Experimental procedures

Sampling, geological settings and dating

A rock salt drill core sample was obtained from the depth of 2026.51–2026.80 m from the northern part of the Qianjiang Depression (30°29′N, 112°58′E) (Fig. 1). The drilling permission (contract number O815091H01) was issued and the drilling was performed by Research Institute of Exploration and Development, Jianghan Oilfield Company, SINOPEC (Jianghan Petroleum Administration Bureau, Guanghua, Qianjiang City, Hubei, China). The sample dating was carried out using a method described here in brief (Košler *et al*., 2002). Heavy liquid and magnetic zircon separation techniques were used to retrieve detrital zircons from the halite (Söderlund and Johansson, 2002). About 200 zircon grains were selected and cast in epoxy. Samples were polished before being photographed under reflected and transmitted light. Images of zircon grains were obtained by cathodoluminescence spectroscopy (MonoCL4+, Gatan). A total of 11 zircons were selected for U-Pb and trace element analysis by LA-ICP-MS (Liu *et al*., 2008). The analysis of the data was conducted by ICPMSDATACAL 8.4 software (Liu *et al*., 2010). Concordia diagrams and weighted mean calculations were made using ISOPLOT 3.00 (Ludwig, 2003).

Surface sterilization of the crystal, and microscopy of the samples

Crystal surface sterilization using 10 M NaOH and HCl (Jaakkola *et al*., 2014), plating and strain isolation were conducted in a cell cultivation room with an entry chamber, which had not been used for handling of halophiles. A clean set of protective clothing was used by researchers entering the room. The laminar flow hood used for crystal and microbe handling was cleaned with antimicrobial solution [1.5 % (v/v) Barrydin, PAN Biotech GmbH] and 70% (v/v) ethanol in succession. All solutions and equipment were autoclaved before use, and their sterility was confirmed by plating using modified growth medium (MGM) plates (see next section on Media and cultivation of the cells), and incubated for up to 3 months at 37°C.

A crystal sample of 53.20 g was selected for microbiological studies (Fig. S2A). After surface sterilization, the crystal was cut in half and final isolation samples were chiselled off from the fresh crystal surface and placed into sterile preweighed tubes. Some of the samples cut from the surface-sterilized salt crystals were examined by light microscopy (Nikon SMZ745T microscope, Jenoptik ProgRes SpeedXT core 3 camera) to visualize crystal structure and liquid inclusions.

Media, cultivation of the cells and virus screening

Two separate aliquots of the isolation sample were dissolved [1 g of sample to 1 ml of 20% (w/v) artificial salt water (SW)] and spread on MGM plates [20% (w/v) SW] using sterile disposable equipment (Dyall-Smith, 2009; Holmes and Dyall-Smith, 1990; Nuttall and Dyall-Smith, 1993). Plates were incubated for up to 3 months at 37°C in aerobic conditions. New plastic boxes with lids were used to protect the plates from drying and external contaminants, and cups of sterile water were kept inside the boxes to maintain humidity. Obtained colonies were purified by three consecutive platings of a single colony, and the purified isolates were named numerically from JI20-1 to JI20-8. MGM broth [23% (w/v) SW] was used for cell cultivation in liquid (Dyall-Smith 2009; Holmes and Dyall-Smith, 1990).

For growth condition optimization, JI20-1 cells were grown in modified MGM broth with different Na^+ or Mg^{2+} concentrations (in 0.5 intervals from 0 to 4.5 M, and in 0.1 intervals from 0 to 0.6 M respectively) at 40°C. For growth temperature optimization, JI20-1 cells were grown on MGM plates at 22, 30, 40, 50 and 55°C and at 37, 40, 45 and 50°C in modified MGM broth with 2.5 M Na^+ and 0.1 M Mg^{2+}. For DNA isolation and microscopy, the cells were grown in modified MGM broth with 2.5 M Na^+ and 0.1 M Mg^{2+} at 45°C.

Virus screening was carried out using halite samples that had been dissolved in SW as previously described, and filtered (0.2 μm). A mixture of 100 μl of the filtered sample, 300 μl of cell culture and 3 ml of top-layer MGM agar [18% (w/v) SW] (Dyall-Smith 2009; Holmes and Dyall-Smith, 1990; Nuttall and Dyall-Smith, 1993) were used per plate, and the plates were incubated at 37°C. Cells used here included *Hbt. hubeiense* JI20-1, which was isolated in this study, *Halobacterium* sp. YI80-1 and YI80-2 (Jaakkola *et al*., 2014), and *Halolamina* sp. YI80-3 to YI80-8 (Jaakkola *et al*., 2014). All cells here were grown in MGM at 37°C.

Electrophoresis of whole cell proteins and microscopy of the cells

Sodium dodecyl sulfate polyacrylamide gel electrophoresis (SDS-PAGE) was used to separate proteins of entire cells [14% (v/v) acrylamide] (Olkkonen and Bamford, 1989; Hantula *et al*., 1990). The gel was stained with Coomassie blue.

JI20-1 cells at late logarithmic phase (A_{550} 0.7–0.8) were examined by light microscopy (Olympus BX50F-3). Thin section samples for transmission electron microscopy (80 kV, JEOL 1200Ex) of JI20-1 cells were prepared and imaged at the Electron Microscopy Unit of the Institute of Biotechnology, Helsinki University (Bamford and Mindich, 1980).

DNA extraction

Cells were collected, re-suspended 1:40 in buffer (10 mM Tris-HCl, 1 mM ethylenediaminetetraacetic acid, pH 8.0; TE buffer) and frozen at –20°C. The suspension was thawed at 22°C for 1 h in the presence of lysozyme (Sigma, final concentration of 2 mg ml^{-1}). SDS [final 0.7% (w/v)] and proteinase K (Roche, final 0.15 mg ml^{-1}) were added to the cells, followed by incubation at 37°C for 30 min and then at 4°C overnight. DNA was extracted with phenol, precipitated with Na-acetate (final 0.3 M) and ethanol [final 64% (v/v)], collected by centrifugation and re-suspended in TE buffer. The sample was incubated overnight at 4°C with the addition of RNase cocktail [Invitrogen, final 0.002% (v/v)]. A second extraction was carried out by using phenol-chloroform (2:1) and chloroform. DNA was precipitated as above. Residual salts were removed by 70% (v/v) ethanol. The DNA was dried and re-suspended in sterile water, and its quality and concentration were determined photometrically.

Genome sequencing, assembly and annotation

Sequencing and assembly of the complete JI20-1 genome and draft genomes of JI20-2 to JI20-8 were carried out at Beijing Genomics Institute, Hong Kong. Polymerase chain reaction (PCR)-free libraries of 500 bp and index libraries of 2000 bp and 6000 bp were used for genome sequencing (Illumina Genome Analyzer, Solexa). The reads were assembled using the SOAPdenovo 1.05 software (Li *et al*., 2010). Contig graphs were built with paired-end reads mapping position. To determine the complete JI20-1 genome sequence, local assembly and gap closure were performed using paired-end reads, and PCR gap closure for unassembled regions. SOAPaligner/soap2 software (Li *et al*., 2009) was used for quality control of the assembly.

Glimmer 3.0 was used for initial gene prediction (Delcher *et al*., 1999; 2007), ACLAME database (Leplae *et al*., 2004) and Standalone BLAT v. 34 (http://genome.ucsc.edu/) (Kent, 2002) for prophage prediction and CRISPRFinder for identifying CRISPR sequences (Grissa *et al*., 2007b). Non-coding RNA was predicted with rRNAmmer, tRNAscan and Bcheck (Schattner *et al*., 2005; Lagesen *et al*., 2007; Yusuf *et al*., 2010). Mobile genetic elements were assigned by iterative tBLASTn of the *Hbt. hubeiense* genome against a manually curated set of mobile genetic elements from the collection of haloarchaea (Dyall-Smith *et al*., 2011).

A set of manually curated haloarchaeal genomes in HaloLex (https://www.halolex.mpg.de/) (*Hbt. salinarum* R1, *Nmn. pharaonis*, *Nmn. moolpensis*, *Hqr. walsbyi* strains HBSQ001 and C23, *Hfx. volcanii*, *Hfx. mediterranei*, *Har. marismortui*, *Har. hispanica* and *Nab. magadii*) was used for validation and improving the quality of the initial prediction of RNA- and protein-coding genes (Pfeiffer *et al*., 2008a). Initial function assignments for the predicted genes were also cross-validated against this set (Falb *et al*., 2008; Pfeiffer *et al*., 2008a). The protein names, gene names and Enzyme Commission (EC) numbers in this genome set are regularly cross-validated against UniProt. As a fundamental curation principle, an attempt is made to identify experimentally characterized homologues and use them for homology-based function assignment (Pfeiffer *et al*., 2008a).

Genes that were not found in the initial prediction were identified by searching for protein-coding genes from the curated halophile set that score the higher with tBLASTn against the *Hbt. hubeiense* genome, compared to BLASTp against the initial *Hbt. hubeiense* ORF set. The newly predicted genes were subsequently generated using a six-frame translator in HaloLex (Pfeiffer *et al*., 2008a). Pseudogenes were handled manually, commonly by tBLASTn analysis comparing a closely related complete homologue against the *Hbt. hubeiense* genome and subsequent setting of ORF termini. The complete genome was manually inspected for atypical gene overlaps using HaloLex. Atypical gene overlaps were manually resolved.

Phylogenetic tree construction

The alignment of 16S rRNA and *rpoB′* gene sequences was performed with ClustalW (Larkin *et al*., 2007). Maximum likelihood and maximum parsimony phylogenetic trees were generated by Molecular Evolutionary Genetics Analysis (MEGA) software version 5.05, with 1000 bootstrap samplings (Tamura *et al*., 2011).

DNA–DNA hybridization

Spectroscopic whole genomic DNA–DNA hybridization between isolate JI20-1 and *Hbt. noricense* (DSM 15987) (Gruber *et al*., 2004) was carried out by Deutsche Sammlung von Microorganismen und Zellkulturen (DSMZ). Cells were disrupted by using a Constant Systems TS 0.75 KW (IUL Instruments, Germany). DNA in the crude lysate was purified by chromatography on hydroxyapatite (Cashion *et al*., 1977). DNA–DNA hybridization was carried out as previously

described (Ley *et al*., 1970) under consideration of modifications (Huss *et al*., 1983) using a model Cary 100 Bio UV/VIS-spectrophotometer equipped with *in situ* temperature probe (Varian).

Identification of most closely related organisms

Searching UniProt (release 2014_07) for the term 'Halobacteriaceae' resulted in 379 147 entries. UniProt codes have organism tags that may be specific (e.g. _HALVD for *Haloferax volcanii*) or general (e.g. _9EURY). Specific organism tags with large-scale data (more than 1000 entries) were considered to represent complete (or draft) genomes. From the general tag category, only _9EURY was selected, as it contains species with large-scale data. Entries from complete genomes (377 056) were extracted, based on identification by their specific organism tag or their species name. The extracted entries formed a database representing 102 complete haloarchaeal proteomes. Each of the *Hbt. hubeiense* protein-coding genes was compared with this database using BLASTp. Only hits with an e-value better than e-20 were preserved. Best BLASTp hit analysis may be misleading when there are only marginal sequence differences between proteins from different organisms. To overcome this problem, top-scoring homologues that had a BLASTp score reaching at least 80% of the best score were selected. The top-scoring homologous ORFs were counted and the proteome coverage (percentage of reference strain ORFs with top-scoring homologues in *Hbt. hubeiense*) was computed.

Acknowledgements

We thank Research Institute of Exploration and Development, Jianghan Oilfield Company, SINOPEC for their contribution. This work was supported by Academy Professor (Academy of Finland) funding grants (grant numbers 255342, 283072) to D.B.H.) and received grants from the National Basic Research Program of China (973 Program) no. 2011CB808800. The authors state no conflict of interest.

The JI20-1 - JI20-8 genome sequences are deposited to European Nucleotide Archive and available the ENA browser at http://www.ebi.ac.uk/ena/data/view/<ACCESSION NUMBERS>. Accession numbers are LN831302-LN831305 (for JI20-1), CEMO01000001-CEMO01000010 (for JI20-2), CEMN01000001-CEMN01000016 (for JI20-3), CEML 01000001-CEML01000018 (for JI20-4), CEMR01000001-CEMR01000015 (for JI20-5), CEMP01000001-CEMP 01000010 (for JI20-6), CEMQ01000001-CEMQ01000012 (for JI20-7), and CEMZ01000001-CEMZ01000011 (JI20-8). The data for JI20-1 are part of the bioproject PRJEB4726.

Halobacterium hubeiense JI20-1 to JI20-8 strains are deposited to HAMBI culture collection (HAMBI 3616 to HAMBI 3623, in numerical order).

References

Anderson, K.L., Apolinario, E.E., and Sowers, K.R. (2012) Desiccation as a long-term survival mechanism for the archaeon *Methanosarcina barkeri*. *Appl Environ Microbiol* **78:** 1473–1479.

Asgarani, E., Funamizu, H., Saito, T., Terato, H., Ohyama, Y., Yamamoto, O., and Ide, H. (1999) Mechanisms of DNA protection in *Halobacterium salinarium*, an extremely halophilic bacterium. *Microbiol Res* **154:** 185–190.

Atanasova, N.S., Roine, E., Oren, A., Bamford, D.H., and Oksanen, H.M. (2012) Global network of specific virus–host interactions in hypersaline environments. *Environ Microbiol* **14:** 426–440.

Baliga, N.S., Bjork, S.J., Bonneau, R., Pan, M., Iloanusi, C., Kottemann, M.C., *et al*. (2004) Systems level insights into the stress response to UV radiation in the halophilic archaeon *Halobacterium* NRC-1. *Genome Res* **14:** 1025–1035.

Bamford, D.H., and Mindich, L. (1980) Electron microscopy of cells infected with nonsense mutants of bacteriophage φ6. *Virology* **107:** 222–228.

Beauheim, R.L., and Roberts, R.M. (2002) Hydrology and hydraulic properties of a bedded evaporite formation. *J Hydrol* **259:** 66–88.

Berquist, B.R., and DasSarma, S. (2003) An archaeal chromosomal autonomously replicating sequence element from an extreme halophile, *Halobacterium* sp. Strain NRC-1. *J Bacteriol* **185:** 5959–5966.

Bidle, K.D., Lee, S., Marchant, D.R., and Falkowski, P.G. (2007) Fossil genes and microbes in the oldest ice on Earth. *Proc Natl Acad Sci* **104:** 13455–13460.

Breuert, S., Allers, T., Spohn, G., and Soppa, J. (2006) Regulated polyploidy in halophilic archaea. *PLoS ONE* **1:** e92.

Cano, R.J., and Borucki, M.K. (1995) Revival and identification of bacterial spores in 25- to 40-million-year-old Dominican amber. *Science* **268:** 1060–1064.

Cashion, P., Holder-Franklin, M., McCully, J., and Franklin, M. (1977) A rapid method for the base ratio determination of bacterial DNA. *Anal Biochem* **81:** 461–466.

Castello, J.D., Rogers, S.O., Starmer, W.T., Catranis, C.M., Ma, L., Bachand, G.D., *et al*. (1999) Detection of tomato mosaic tobamovirus RNA in ancient glacial ice. *Polar Biol* **22:** 207–212.

Christner, B.C., Mosley-Thompson, E., Thompson, L.G., and Reeve, J.N. (2003) Bacterial recovery from ancient glacial ice. *Environ Microbiol* **5:** 433–436.

da Costa, M.S., Santos, H., and Galinski, E.A. (1998) An overview of the role and diversity of compatible solutes in Bacteria and Archaea. In *Biotechnology of Extremophiles*. Antranikian, G. (ed.). Berlin, Germany: Springer Berlin Heidelberg, pp. 117–153.

DasSarma, S., Halladay, J.T., Jones, J.G., Donovan, J.W., Giannasca, P.J., and de Marsac, N.T. (1988) High-frequency mutations in a plasmid-encoded gas vesicle gene in *Halobacterium halobium*. *Proc Natl Acad Sci* **85:** 6861–6865.

Delcher, A.L., Harmon, D., Kasif, S., White, O., and Salzberg, S.L. (1999) Improved microbial gene identification with GLIMMER. *Nucleic Acids Res* **27:** 4636–4641.

Delcher, A.L., Bratke, K.A., Powers, E.C., and Salzberg, S.L. (2007) Identifying bacterial genes and endosymbiont DNA with Glimmer. *Bioinformatics* **23:** 673–679.

DeMaere, M.Z., Williams, T.J., Allen, M.A., Brown, M.V., Gibson, J.A., Rich, J., *et al*. (2013) High level of intergenera gene exchange shapes the evolution of

haloarchaea in an isolated Antarctic lake. *Proc Natl Acad Sci* **110:** 16939–16944.

Denner, E.B.M., McGenity, T.J., Busse, H.-J., Grant, W.D., Wanner, G., and Stan-Lotter, H. (1994) *Halococcus salifodinae* sp. nov., an archaeal isolate from an Austrian salt mine. *Int J Syst Bacteriol* **44:** 774–780.

DeVeaux, L.C., Müller, J.A., Smith, J., Petrisko, J., Wells, D.P., and DasSarma, S. (2007) Extremely radiation-resistant mutants of a halophilic archaeon with increased single-stranded DNA-binding protein (RPA) gene expression. *Radiat Res* **168:** 507–514.

Du, C., Yang, C., Yao, Y., Li, Z., and Chen, J. (2012) Mechanical behavior of deep rock salt under the operational conditions of gas storage. *Int J Earth Sci Eng* **5:** 1670–1676.

Dyall-Smith, M.L. (2009) Halohandbook [WWW document]. URL www.haloarchaea.com/resources/halohandbook.

Dyall-Smith, M.L., Pfeiffer, F., Klee, K., Palm, P., Gross, K., Schuster, S.C., *et al*. (2011) *Haloquadratum walsbyi*: limited diversity in a global pond. *PLoS ONE* **6:** e20968.

Dyall-Smith, M.L., Pfeiffer, F., Oberwinkler, T., Klee, K., Rampp, M., Palm, P., *et al*. (2013) Genome of the haloarchaeon *Natronomonas moolapensis*, a neutrophilic member of a previously haloalkaliphilic genus. *Genome Announc* **1:** e00095-00013.

Falb, M., Müller, K., Königsmaier, L., Oberwinkler, T., Horn, P., Gronau, S., *et al*. (2008) Metabolism of halophilic archaea. *Extremophiles* **12:** 177–196.

Fendrihan, S., Leuko, S., and Stan-Lotter, H. (2004) Effects of embedding *Halobacterium* sp. NRC-1 in salt crystals and potential implications for long term preservation. *Proceed Third Eur Workshop Exo-Astrobiol* **545:** 203–204.

Fendrihan, S., Bérces, A., Lammer, H., Musso, M., Rontó, G., Polacsek, T.K., *et al*. (2009) Investigating the effects of simulated Martian ultraviolet radiation on *Halococcus dombrowskii* and other extremely halophilic archaebacteria. *Astrobiology* **9:** 104–112.

Fendrihan, S., Dornmayr-Pfaffenhuemer, M., Gerbl, F.W., Holzinger, A., Grösbacher, M., Briza, P., *et al*. (2012) Spherical particles of halophilic archaea correlate with exposure to low water activity – implications for microbial survival in fluid inclusions of ancient halite. *Geobiology* **10:** 424–433.

Fish, S.A., Shepherd, T.J., McGenity, T.J., and Grant, W.D. (2002) Recovery of 16S ribosomal RNA gene fragments from ancient halite. *Nature* **417:** 432–436.

Gramain, A., Díaz, G.C., Demergasso, C., Lowenstein, T.K., and McGenity, T.J. (2011) Archaeal diversity along a subterranean salt core from the Salar Grande (Chile). *Environ Microbiol* **13:** 2105–2121.

Grant, W.D., Gemmell, R.T., and McGenity, T.J. (1998) Halobacteria: the evidence for longevity. *Extremophiles* **2:** 279–287.

Greenblatt, C.L., Davis, A., Clement, B., Kitts, C., Cox, T., and Cano, R.J. (1999) Diversity of microorganisms isolated from amber. *Microb Ecol* **38:** 58–68.

Greenblatt, C.L., Davis, A., Clement, B.G., Kitts, C.L., Cox, T., and Cano, R.J. (1999) Diversity of microorganisms isolated from amber. *Microb Ecol* **38:** 58–68.

Greenblatt, C.L., Baum, J., Klein, B.Y., Nachshon, S., Koltunov, V., and Cano, R.J. (2004) *Micrococcus luteus* – survival in amber. *Microb Ecol* **48:** 120–127.

Grissa, I., Vergnaud, G., and Pourcel, C. (2007a) The CRISPRdb database and tools to display CRISPRs and to generate dictionaries of spacers and repeats. *BMC Bioinformatics* **8:** 172.

Grissa, I., Vergnaud, G., and Pourcel, C. (2007b) CRISPRFinder: a web tool to identify clustered regularly interspaced short palindromic repeats. *Nucleic Acids Res* **35:** W52–W57.

Gruber, C., Legat, A., Pfaffenhuemer, M., Radax, C., Weidler, G., Busse, H.-J., and Stan-Lotter, H. (2004) *Halobacterium noricense* sp. nov., an archaeal isolate from a bore core of an alpine Permian salt deposit, classification of *Halobacterium* sp. NRC-1 as a strain of *H. salinarum* and emended description of *H. salinarum*. *Extremophiles* **8:** 431–439.

Hantula, J., Korhonen, T.K., and Bamford, D.H. (1990) Determination of taxonomic resolution capacity of conventional one-dimensional SDS-polyacrylamide gel electrophoresis of whole-cell proteins using *Enterobacteriaceae*. *FEMS Microbiol Lett* **70:** 325–330.

Holmes, M.L., and Dyall-Smith, M.L. (1990) A plasmid vector with a selectable marker for halophilic archaebacteria. *J Bacteriol* **172:** 756–761.

Huss, V.A., Festl, H., and Schleifer, K.H. (1983) Studies on the spectrophotometric determination of DNA hybridization from renaturation rates. *Syst Appl Microbiol* **4:** 184–192.

Jaakkola, S.T., Zerulla, K., Guo, Q., Liu, Y., Ma, H., Yang, C., *et al*. (2014) Halophilic archaea cultivated from surface sterilized middle-late Eocene rock salt are polyploid. *PLoS ONE* e110533.

Johnson, S.S., Hebsgaard, M.B., Christensen, T.R., Mastepanov, M., Nielsen, R., Munch, K., *et al*. (2007) Ancient bacteria show evidence of DNA repair. *Proc Natl Acad Sci* **104:** 14401–14405.

Kent, W.J. (2002) BLAT – the BLAST-like alignment tool. *Genome Res* **12:** 656–664.

Kminek, G., Bada, J.L., Pogliano, K., and Ward, J.F. (2003) Radiation-dependent limit for the viability of bacterial spores in halite fluid inclusions and on Mars. *Radiat Res* **159:** 722–729.

Kokoeva, M.V., Storch, K.F., Klein, C., and Oesterhelt, D. (2002) A novel mode of sensory transduction in archaea: binding protein-mediated chemotaxis towards osmoprotectants and amino acids. *EMBO J* **21:** 2312–2322.

Košler, J., Fonneland, H., Sylvester, P., Tubrett, M., and Pedersen, R.-B. (2002) U–Pb dating of detrital zircons for sediment provenance studies – a comparison of laser ablation ICPMS and SIMS techniques. *Chem Geol* **182:** 605–618.

Kottemann, M., Kish, A., Iloanusi, C., Bjork, S., and DiRuggiero, J. (2005) Physiological responses of the halophilic archaeon *Halobacterium* sp. strain NRC1 to desiccation and gamma irradiation. *Extremophiles* **9:** 219–227.

Lagesen, K., Hallin, P., Rødland, E.A., Stærfeldt, H.-H., Rognes, T., and Ussery, D.W. (2007) RNAmmer: consistent and rapid annotation of ribosomal RNA genes. *Nucleic Acids Res* **35:** 3100–3108.

Lambert, L., Cox, T., Mitchell, K., Rosselló-Mora, R., Del Cueto, C., Dodge, D., *et al*. (1998) *Staphylococcus succinus* sp. nov., isolated from Dominican amber. *Int J Syst Bacteriol* **48:** 511–518.

Larkin, M., Blackshields, G., Brown, N., Chenna, R., McGettigan, P.A., McWilliam, H., *et al*. (2007) Clustal W and Clustal X version 2.0. *Bioinformatics* **23:** 2947–2948.

Legendre, M., Bartoli, J., Shmakova, L., Jeudy, S., Labadie, K., Adrait, A., *et al*. (2014) Thirty-thousand-year-old distant relative of giant icosahedral DNA viruses with a pandoravirus morphology. *Proc Natl Acad Sci* **111:** 4274–4279.

Leplae, R., Hebrant, A., Wodak, S.J., and Toussaint, A. (2004) ACLAME: a classification of mobile genetic elements. *Nucleic Acids Res* **32:** D45–D49.

Ley, J.D., Cattoir, H., and Reynaerts, A. (1970) The quantitative measurement of DNA hybridization from renaturation rates. *Eur J Biochem* **12:** 133–142.

Li, R., Yu, C., Li, Y., Lam, T.-W., Yiu, S.-M., Kristiansen, K., and Wang, J. (2009) SOAP2: an improved ultrafast tool for short read alignment. *Bioinformatics* **25:** 1966–1967.

Li, R., Zhu, H., Ruan, J., Qian, W., Fang, X., Shi, Z., *et al*. (2010) De novo assembly of human genomes with massively parallel short read sequencing. *Genome Res* **20:** 265–272.

Liu, Y., Hu, Z., Gao, S., Günther, D., Xu, J., Gao, C., and Chen, H. (2008) *In situ* analysis of major and trace elements of anhydrous minerals by LA-ICP-MS without applying an internal standard. *Chem Geol* **257:** 34–43.

Liu, Y., Gao, S., Hu, Z., Gao, C., Zong, K., and Wang, D. (2010) Continental and oceanic crust recycling-induced melt–peridotite interactions in the Trans-North China orogen: U–Pb dating, Hf isotopes and trace elements in zircons from mantle xenoliths. *J Petrol* **51:** 537–571.

Ludwig, K.R. (2003) User's manual for isoplot 3.00: a geochronological toolkit for Microsoft Excel. [WWW document]. URL books.google.com/books?id=OutNAQAAIAAJ.

Ma, H., Yang, C., Qi, Z., Li, Y., and Hao, R. (2012) Experimental and numerical analysis of salt cavern convergence in ultra-deep bedded formation. *ARMA: Am Rock Mech Assoc* [WWW document; document ID ARMA-2012-392] URL www.onepetro.org/conference-paper/ARMA-2012-392.

Ma, L.-J., Rogers, S.O., Catranis, C.M., and Starmer, W.T. (2000) Detection and characterization of ancient fungi entrapped in glacial ice. *Mycologia* **92:** 286–295.

McCready, S. (1996) The repair of ultraviolet light-induced DNA damage in the halophilic archaebacteria, *Halobacterium cutirubrum*, *Halobacterium halobium* and *Haloferax volcanii*. *Mutat Res/DNA Repair* **364:** 25–32.

McGenity, T.J., Gemmell, R.T., Grant, W.D., and Stan-Lotter, H. (2000) Origins of halophilic microorganisms in ancient salt deposits. *Environ Microbiol* **2:** 243–250.

Marguet, E., and Forterre, P. (1998) Protection of DNA by salts against thermodegradation at temperatures typical for hyperthermophiles. *Extremophiles* **2:** 115–122.

Matzko, J.R. (1995) Geologic factors affecting seismic monitoring in China. In *US Geological Survey Open-file Report*. 1–44. [WWW document] URL pubs.er.usgs.gov/publication/ofr95562

Maughan, H., Birky, C.W., Jr, Nicholson, W.L., Rosenzweig, W.D., and Vreeland, R.H. (2002) The paradox of the 'ancient' bacterium which contains 'modern' protein-coding genes. *Mol Biol Evol* **19:** 1637–1639.

Miteva, V.I., Sheridan, P.P., and Brenchley, J.E. (2004) Phylogenetic and physiological diversity of microorganisms isolated from a deep Greenland glacier ice core. *Appl Environ Microbiol* **70:** 202–213.

Mormile, M.R., Biesen, M.A., Gutierrez, M.C., Ventosa, A., Pavlovich, J.B., Onstott, T.C., and Fredrickson, J.K. (2003) Isolation of *Halobacterium salinarum* retrieved directly from halite brine inclusions. *Environ Microbiol* **5:** 1094–1102.

Naor, A., Lapierre, P., Mevarech, M., Papke, R.T., and Gophna, U. (2012) Low species barriers in halophilic archaea and the formation of recombinant hybrids. *Curr Biol* **22:** 1444–1448.

Nicholson, W.L. (2003) Using thermal inactivation kinetics to calculate the probability of extreme spore longevity: implications for paleomicrobiology and lithopanspermia. *Orig Life Evol Biosph* **33:** 621–631.

Norton, C.F., McGenity, T.J., and Grant, W.D. (1993) Archaeal halophiles (halobacteria) from two British salt mines. *J Gen Microbiol* **139:** 1077–1081.

Nuttall, S.D., and Dyall-Smith, M.L. (1993) Ch2, a novel halophilic archaeon from an Australian solar saltern. *Int J Syst Bacteriol* **43:** 729–734.

Olkkonen, V.M., and Bamford, D.H. (1989) Quantitation of the adsorption and penetration stages of bacteriophage φ6 infection. *Virology* **171:** 229–238.

Paul, S., Bag, S.K., Das, S., Harvill, E.T., and Dutta, C. (2008) Molecular signature of hypersaline adaptation: insights from genome and proteome composition of halophilic prokaryotes. *Genome Biol* **9:** R70.

Pfeifer, F., and Blaseio, U. (1990) Transposition burst of the ISH27 insertion element family in *Halobacterium halobium*. *Nucleic Acids Res* **18:** 6921–6925.

Pfeiffer, F., Broicher, A., Gillich, T., Klee, K., Mejia, J., Rampp, M., and Oesterhelt, D. (2008a) Genome information management and integrated data analysis with HaloLex. *Arch Microbiol* **190:** 281–299.

Pfeiffer, F., Schuster, S., Broicher, A., Falb, M., Palm, P., Rodewald, K., *et al*. (2008b) Evolution in the laboratory: the genome of *Halobacterium salinarum* strain R1 compared to that of strain NRC-1. *Genomics* **91:** 335–346.

Philp, R., and Zhaoan, F. (1987) Geochemical investigation of oils and source rocks from Qianjiang Depression of Jianghan Basin, a terrigenous saline basin, China. *Org Geochem* **11:** 549–562.

Philp, R., Fan, P., Lewis, C., Zhu, H., and Wang, H. (1991) Geochemical characteristics of oils from the Chaidamu, Shanganning and Jianghan Basins, China. *J Southeast Asian Earth Sci* **5:** 351–358.

Powers, D.W., Vreeland, R.H., and Rosenzweig, W.D. (2001) Biogeology: how old are bacteria from the Permian age? *Nature* **411:** 155–156.

Rosenzweig, W.D., Peterson, J., Woish, J., and Vreeland, R.H. (2000) Development of a protocol to retrieve microorganisms from ancient salt crystals. *Geomicrobiol J* **17:** 185–192.

Sankaranarayanan, K., Timofeeff, M.N., Spathis, R., Lowenstein, T.K., and Lum, J.K. (2011) Ancient microbes from halite fluid inclusions: optimized surface sterilization and DNA extraction. *PLoS ONE* **6:** e20683.

Satterfield, C.L., Lowenstein, T.K., Vreeland, R.H., Rosenzweig, W.D., and Powers, D.W. (2005) New evi-

dence for 250 Ma age of halotolerant bacterium from a Permian salt crystal. *Geology* **33:** 265–268.
Schattner, P., Brooks, A.N., and Lowe, T.M. (2005) The tRNAscan-SE, snoscan and snoGPS web servers for the detection of tRNAs and snoRNAs. *Nucleic Acids Res* **33:** W686–W689.
Schubert, B.A., Lowenstein, T.K., and Timofeeff, M.N. (2009) Microscopic identification of prokaryotes in modern and ancient halite, Saline Valley and Death Valley, California. *Astrobiology* **9:** 467–482.
Schubert, B.A., Lowenstein, T.K., Timofeeff, M.N., and Parker, M.A. (2010a) Halophilic archaea cultured from ancient halite, Death Valley, California. *Environ Microbiol* **12:** 440–454.
Schubert, B.A., Timofeeff, M.N., Lowenstein, T.K., and Polle, J.E.W. (2010b) *Dunaliella* cells in fluid inclusions in halite: significance for long-term survival of prokaryotes. *Geomicrobiol J* **27:** 61–75.
Shahmohammadi, H.R., Asgarani, E., Terato, H., Saito, T., Ohyama, Y., Gekko, K., *et al*. (1998) Protective roles of bacterioruberin and intracellular KCl in the resistance of *Halobacterium salinarium* against DNA-damaging agents. *J Radiat Res* **39:** 251–262.
Sheridan, P.P., Miteva, V.I., and Brenchley, J.E. (2003) Phylogenetic analysis of anaerobic psychrophilic enrichment cultures obtained from a Greenland glacier ice core. *Appl Environ Microbiol* **69:** 2153–2160.
Soppa, J. (2006) From genomes to function: haloarchaea as model organisms. *Microbiology* **152:** 585–590.
Soppa, J. (2011) Ploidy and gene conversion in Archaea. *Biochem Soc Trans* **39:** 150.
Soppa, J. (2013) Evolutionary advantages of polyploidy in halophilic archaea. *Biochem Soc Trans* **41:** 339–343.
Söderlund, U., and Johansson, L. (2002) A simple way to extract baddeleyite (ZrO2). *Geochem Geophys Geosyst* **3:** 1 of 7–7 of 7.
Stackebrandt, E., and Goebel, B.M. (1994) Taxonomic note: a place for DNA-DNA reassociation and 16S rRNA sequence analysis in the present species definition in bacteriology. *Int J Syst Bacteriol* **44:** 846–849.
Stan-Lotter, H., Pfaffenhuemer, M., Legat, A., Busse, H., Jr, Radax, C., and Gruber, C. (2002) *Halococcus dombrowskii* sp. nov., an archaeal isolate from a Permian alpine salt deposit. *Int J Syst Evol Microbiol* **52:** 1807–1814.
Tamura, K., Peterson, D., Peterson, N., Stecher, G., Nei, M., and Kumar, S. (2011) MEGA5: molecular evolutionary genetics analysis using maximum likelihood, evolutionary distance, and maximum parsimony methods. *Mol Biol Evol* **28:** 2731–2739.
Vreeland, R.H., Rosenzweig, W.D., and Powers, D.W. (2000) Isolation of a 250 million-year-old halotolerant bacterium from a primary salt crystal. *Nature* **407:** 897–900.
Vreeland, R.H., Straight, S., Krammes, J., Dougherty, K., Rosenzweig, W.D., and Kamekura, M. (2002) *Halosimplex carlsbadense* gen. nov., sp. nov., a unique halophilic archaeon, with three 16S rRNA genes, that grows only in defined medium with glycerol and acetate or pyruvate. *Extremophiles* **6:** 445–452.
Vreeland, R.H., Jones, J., Monson, A., Rosenzweig, W.D., Lowenstein, T.K., Timofeeff, M., *et al*. (2007) Isolation of live Cretaceous (121–112 million years old) halophilic archaea from primary salt crystals. *Geomicrobiol J* **24:** 275–282.
Wagner, D., Schirmack, J., Ganzert, L., Morozova, D., and Mangelsdorf, K. (2013) *Methanosarcina soligelidi* sp. nov., a desiccation-and freeze-thaw-resistant methanogenic archaeon from a Siberian permafrost-affected soil. *Int J Syst Evol Microbiol* **63:** 2986–2991.
Xiang, F., Zhu, L., Wang, C., Zhao, X., Chen, H., and Yang, W. (2007) Quaternary sediment in the Yichang area: implications for the formation of the Three Gorges of the Yangtze River. *Geomorphology* **85:** 249–258.
Yusuf, D., Marz, M., Stadler, P.F., and Hofacker, I.L. (2010) Bcheck: a wrapper tool for detecting RNase P RNA genes. *BMC Genomics* **11:** 432.
Zerulla, K., Chimileski, S., Näther, D., Gophna, U., Papke, R.T., and Soppa, J. (2014) DNA as a phosphate storage polymer and the alternative advantages of polyploidy for growth or survival. *PLoS ONE* **9:** e94819.
Zharkov, M.A. (1981) *History of Paleozoic Salt Accumulation*. Berlin, Germany: Springer.

Supporting information

Additional Supporting Information may be found in the online version of this article at the publisher's web-site:

Fig. S1. Sample dating by U-Pb measurements and laser ablation inductively coupled plasma mass spectrometry. Concordia diagrams showing (A) all of the age populations of zircons (circled areas) in the sample, (B) and the populations aged from 70 to 210 MYA.
Fig. S2. The crystal sample used for microbe isolation (A) after surface sterilization, and (B–D) subsections cut from the crystal examined by light microscopy. Black arrowheads point at cubic liquid inclusions in D.
Fig. S3. Growth curves of (A) JI20-1 at 40°C in modified growth medium (MGM) with different concentrations of NaCl or (B) $MgCl_2$, and (C) in MGM with 2.5 M NaCl, 0.1 M $MgCl_2$ in different temperatures. (D) Growth curves of all JI20 strains in optimized conditions in modified MGM with 2.5 M NaCl, 0.1 M $MgCl_2$, at 45°C.
Fig. S4. Whole cell protein patterns of (A) *Halobacterium noricense* and (B) isolate JI20-1 analysed in Coomassie-stained SDS-PAGE gel. Molecular mass standard is shown on left.
Table S1. U-Pb dating and trace element analysis of zircon grains by laser ablation inductively coupled plasma mass spectrometry.
Table S2. Scaffold data from genome sequencing.
Table S3. *Halobacterium hubeiense* CRISPR spacers with 100% identical hits to viral sequences.